2014 International Conference on Geological and Civil Engineering
IPCBEE vol.62 (2014) © (2014) IACSIT Press, Singapore
DOI: 10.7763/IPCBEE. 2014. V62. 7

Shear Strength of Low-rise RC Walls with Grade 550 MPa Bars

Jang-Woon Baek [1+], Hong-Gun Park [2], and Hyun-Mock Shin [3]

[1, 2] Department of Architecture & Architectural Engineering at Seoul National Univ., South Korea.
[3] Department of Civil Engineering at Sungkyunkwan Univ., South Korea

Abstract. In the construction of nuclear power plants using massive walls, the use of high-strength re-bars for shear design is necessary, to enhance the constructability and economy. In this study, low-rise walls (aspect ratio of 1.0) with Grade 550 MPa re-bars were tested, to investigate the shear capacity under cyclic loading. The test parameters were the grade of horizontal reinforcement, concrete strength, shapes of cross-section. The failure mode of the walls with 550 MPa bars was diagonal shear cracking, followed by web-crushing, which was the same as that of the wall with 420 MPa bars. The ratio of the peak shear strength to the prediction of ACI 349 was 1.33~1.80 for the shear provision, and 1.27~1.69 for the seismic provision, respectively. The test result indicates that Grade 550 MPa re-bars can be applicable to low-rise RC walls.

Keywords: low aspect ratio, shear strength, high-strength re-bars, structural wall, cyclic loading

1. Introduction

Generally in nuclear power plant walls, because of the high safety requirement, the shear reinforcement ratio is close to the permissible maximum shear reinforcement ratio specified by current design codes. According to Chapter 11 of ACI 318-11 [1] and ACI 349-06 [2], the maximum shear strength of flexural members (i.e. the sum of the contributions of concrete and shear reinforcement) is specified to control shear crack widths, and to prevent early diagonal concrete crushing. Currently, the average ultimate shear stress in a cross-section is limited to $5/6\sqrt{f_c'}$ for flexural members including walls. When high strength bars are considered for shear reinforcement, the validity of the maximum shear strength limitation needs to be verified. In the present study, cyclic lateral loading tests were performed for low-rise walls ($h_w / l_w \le 1.0$) with Grade 550 MPa bars, to investigate the shear strength before flexural yielding. The test results were compared with the shear strengths predicted by current design codes. On the basis of the results, the effect of Grade 550 MPa bars on the structural performance of low-rise walls ($h_w / l_w \le 1.0$) was discussed.

2. Experimental Program

2.1. Major Test Parameters

As mentioned, in nuclear power plant walls, the shear reinforcement ratio is close to the permissible maximum shear reinforcement ratio specified by current design codes. Thus, the permissible maximum shear reinforcement ratio was used for the major test parameter, focusing on the behavior of walls with high shear reinforcement ratio.

In ACI 349 (ACI 318), the shear strength of walls is defined as the sum of the contributions of concrete V_c, and shear reinforcement V_s:

$$V_n = V_c + V_s \tag{1}$$

$$V_c = \left(\sqrt{f_c'} / 6\right) hd \tag{2a}$$

$$V_c = 0.28\sqrt{f_c'}\, hd + N_u d \big/ 4l_w \text{, or} \tag{2b}$$

[+] Corresponding author. Tel.: + 82-2-880-7053; fax: +82-2-882-7053.
E-mail address: baekja1@snu.ac.kr.

$$V_c = \left[0.05\sqrt{f_c^{'}} + l_w\left(0.10\sqrt{f_c^{'}} + 0.2N_u/(l_w h)\right)\Big/\left(M_u/V_u - l_w/2\right)\right]hd \quad (2c)$$

$$V_s = A_v f_{yh} d/s \quad (3)$$

Where, $f_c^{'}$ = cylinder strength of concrete, l_w = length of wall, h = thickness of wall, d = distance from the extreme compression fiber to the centroid of longitudinal tension reinforcement (= $0.8l_w$ in ACI 349), V_u = applied shear force, N_u = axial force (positive sign in compression), and A_v = area of shear reinforcement within spacing s.

On the other hand, in the seismic provisions of ACI 349 (ACI 318), the shear strength of walls is specified as follows.

$$V_n \le A_{cv}\left(\alpha_c\sqrt{f_c^{'}} + \rho_t f_y\right) \quad (4)$$

The first term in the right hand side indicates V_c, and the second term indicates V_s. In Eq. (4), A_{cv} is the total sectional area, and the coefficient α_c is 0.25 for $h_w/l_w \le 1.5$

In the general and seismic provisions, the permissible maximum shear strength is specified as follows.

$$V_n \le 5/6\sqrt{f_c^{'}}hd\left(= 2/3\sqrt{f_c^{'}}A_{cv}\right) \quad (5)$$

Where $A_{cv} = hl_w$ and $d = 0.8l_w$. Thus, the permissible maximum shear strength of web horizontal bars can be defined as follows.

$$V_{smax} = 5/6\sqrt{f_c^{'}}hd - V_c \quad (6)$$

In case of the control specimen **S1**, $f_c^{'}$ = 46 MPa, l_w =200 mm, and d = 1200 mm. In the design of **S1**, Eq. (2c) was selected to calculate V_c, which was 557 kN. Thus, the permissible maximum shear strength provided by shear reinforcement was calculated as V_{smax} = 800 kN (V_{smax} = 1,085 kN for Eq. (2a), 707 kN for Eq. (2b), and 850 kN for Eq. (4)).

Four wall specimens with aspect ratio of 1.0 were prepared for testing (Fig. 1, and Table 1). In the control specimen **S1**, the permissible maximum shear strength was used to design the web horizontal bars: V_s = V_{smax} (= 800 kN). For the horizontal bars, Grade 550 MPa D13 (nominal diameter = 13 mm, A_v =126.7 mm^2) was used. The actual yield strength was f_{yh} =667 MPa. Using Eq. (3) and the actual yield strength, the ratio and spacing of the horizontal bars were determined as ρ_h =0.0051 and s = 250 mm. The design value ρ_h =0.0051 is significantly less than the maximum reinforcement ratio that is used in practice for the design of nuclear power plant walls. This is because, 1) the bar grade was increased from 420MPa to 550MPa, and 2) the actual yield strength f_{yh} =667 MPa was much greater than the specified yield strength, and 3) for the calculation of V_c, Eq. (2c) was used: V_c in Eq. (2c) is greater than V_c in the simplified equation Eq. (2a).

For direct comparison between Grade 550 and 420 MPa bars, Specimen **S2** using Grade 420 MPa bars was designed with a higher horizontal bar ratio ρ_h =0.0068, which was about 1.3 (= 550/420) times ρ_h =0.0051 of **S1**.

In specimens **S3** and **S4**, in which 70 MPa concrete and a barbell shape cross-section were used, respectively, ρ_h =0.0051 was used for the horizontal bar ratio, which was the same as that of **S1**. Table 1 presents the details used for the specimens.

Table 1: Design Parameters of test specimens

Specimen	Failure mode	Sectional shape	Compressive strength $f_c^{'}$ MPa	Wall web region					Wall boundary region		
				Horizontal			Vertical		Confinement re-bars	Vertical	
				V_s/V_{smax}	f_{yh} MPa	ρ_h (%)	f_{yv} MPa	ρ_v (%)		f_{yf} MPa	ρ_f (%)
S1	shear	rectangle	46.5	1.01	667	0.51	653	0.66	-	617	9.7
S2	shear	rectangle	46.5	0.95	445	0.68	653	0.66	-	617	9.7
S3	shear	rectangle	70.3	0.89	667	0.51	653	0.66	-	617	9.7
S4	shear	barbell	46.5	0.87	667	0.51	653	0.54	D13 at 55	617	9.7

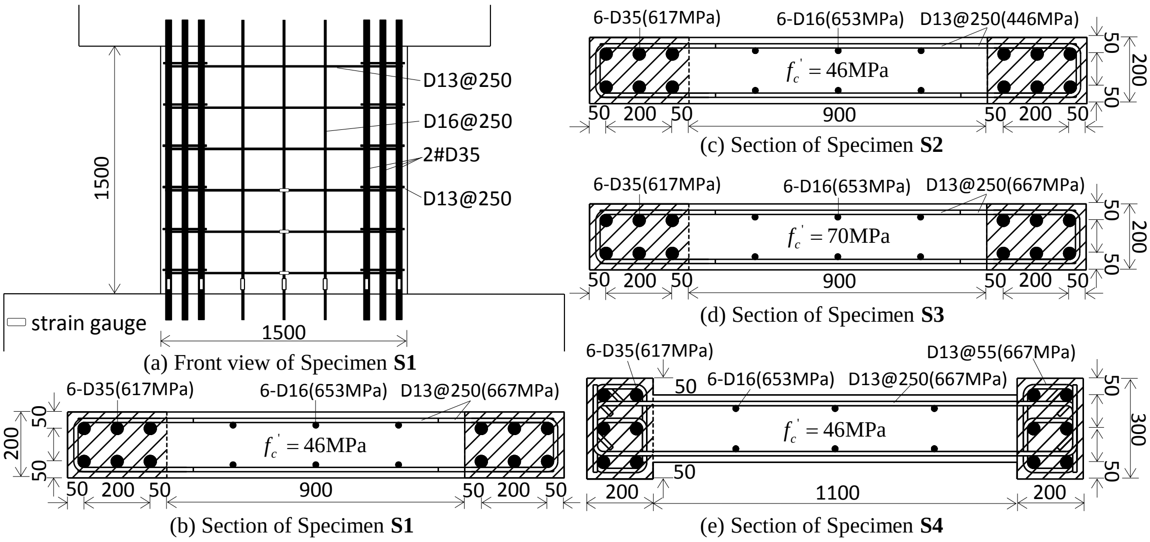

Fig. 1: Dimension and reinforcement details of specimens.

2.2. Test Procedure and Instrumentation

Axial compressive loading and lateral cyclic loading were applied. An axial load of approximately $0.07 A_c f_c'$ (970 kN for 46 MPa concrete (**S1** and **S2**), 1,470 kN for 70 MPa concrete (**S3**), and 1,150 kN for **S4**), was applied at the top of the wall by two UTMs. The lateral loading protocol followed the “Acceptance Criteria for Special Structural Walls” [3].

3. Test Results

Fig. 2 shows the lateral load-displacement (story drift ratio) relationships of the test specimens. This figure also shows the shear strength and flexural strength predicted by ACI 349 (ACI 318). As expected, the peak strength did not reach the predicted flexural strength, which indicates that the measured maximum lateral load V_{test} was determined by shear failure.

In Specimen **S1** (Fig. 2 (a)), with the permissible maximum horizontal bar ratio (f_{yh} =667 MPa, ρ_h =0.0051) and 46 MPa concrete, the load-carrying capacity gradually increased with the lateral displacement. Then, the load suddenly decreased at the story drift ratio of 1.0%. The maximum strength V_{test} was +2,187 and -2,129 kN in the positive and negative loading directions, respectively.

The load-displacement relationship of **S2** with Grade 420 horizontal bars (f_{yh} =446 MPa, ρ_h =0.0068) was similar to that of **S1** with Grade 550 MPa horizontal bars. The failure of the specimen occurred at the story drift ratio of 1.00~1.25% (Fig. 2 (b)). The maximum strength V_{test} was +2,331 and -2,265 kN, which was on average 7% greater than that of **S1**.

In **S3** (Fig. 2 (c)) with 70 MPa concrete and Grade 550 MPa horizontal bars, the failure of the specimen occurred at the story drift of 0.75%, which was less than that of **S1**. The maximum strength V_{test} was +2,035 and -2,135 kN. This result indicates that the shear strength did not increase, despite the use of high-strength concrete. However, the shear strength was greater than the predicted shear strength, and the permissible maximum shear strength specified in ACI 349: $V_{max} = 5/6\sqrt{f_c'}hd$ = 1,673 kN.

In **S4** (Fig. 2 (d)) with barbell type cross-section, the failure occurred at the story drift ratio of 1.25%. Due to the effect of the boundary elements, the maximum strength V_{test} was increased to +2,579 and -2,510 kN, which were on average 17% greater than that of **S1**.

Fig. 3 shows the damage modes of specimens at the peak loads. In **S1, S2,** and **S3** without boundary confinement, after diagonal macro-cracks developed, sliding of the upper part of the panel occurred along the diagonal crack (Fig. 3 (a), (b), and (c)). As the sliding progressed, ultimately, concrete crushing/spalling occurred in the web. On the other hand, in **S4**, boundary confinement restrained the propagation of diagonal macro-cracks to the boundary zones. Thus, ultimately, web concrete crushing occurred without sliding of the panel and crushing at the wall bottom (Fig. 3 (d)). In all specimens, at least one of the horizontal bars yielded before the failure of the walls according to the measured strain data.

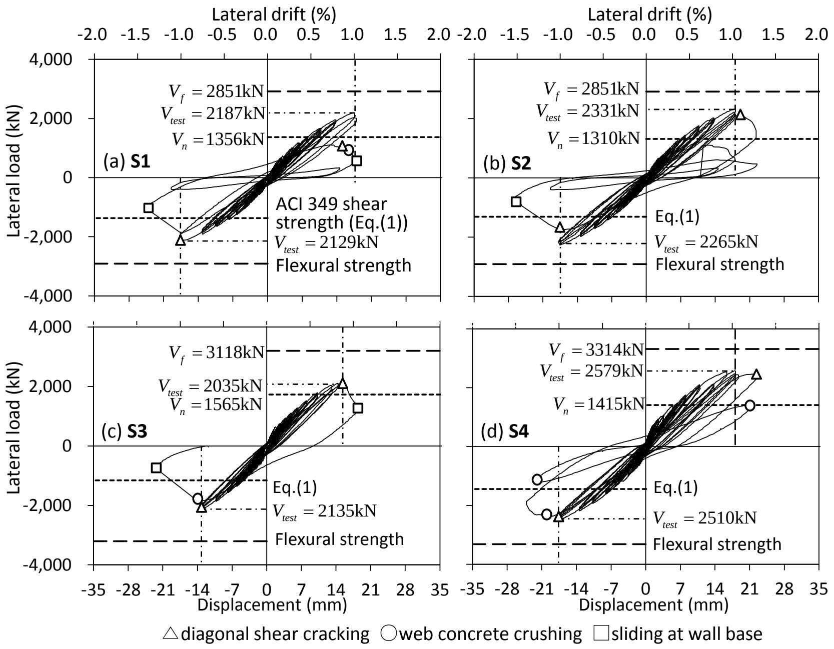

Fig. 2: Lateral load-displacement relationships of specimens.

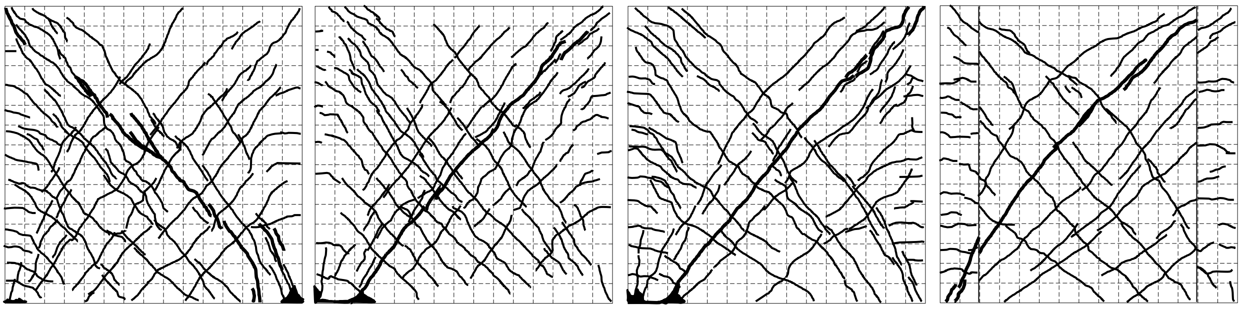

(a) Specimen S1 (b) Specimen S2 (c) Specimen S3 (d) Specimen S4

Fig. 3: Damage modes of specimens at peak load.

4. Comparisons of Shear Predictions

Table 2 compares the ACI 349 shear strengths V_n (general provision) and V_{seis} (seismic provision), Eurocode 8 [4] shear strength V_{RD}, empirical equation V_{Wh} proposed by Gulec and Whittaker [5], and maximum strength predicted by nonlinear finite element analysis V_{FE}.

Table 2: Comparison of shear strengths predicted by current design codes

Specimen	V_f kN	Test results			Ratio of test strength to predictions				
		V_{test} kN	Drift at V_{test} %	Failure mode	ACI 349 Shear provision V_{test}/V_n	ACI 349 Seismic provision V_{test}/V_{seis}	Eurocode8 V_{test}/V_{RD}	Shear prediction by Whittaker V_{test}/V_{Wh}	FE analysis V_{test}/V_{FE}
S1	2,914	2,158	1.00	WCS	1.59	1.59	2.23	1.27	1.01
S2	2,914	2,298	1.00		1.75	1.69	2.37	1.36	1.00
S3	3,200	2,085	0.75		1.33	1.27	1.72	1.00	0.88
S4	3,142	2,544	1.00	WC	1.80	1.53	2.63	1.08	1.02

Notes: V_f = flexural strength predictions, V_{test} = the average value of the measured maximum loads in positive and negative loading directions. V_n = shear for Eq.(1), (2c), (3), and V_{seis} = shear for Eq. (4). WCS is web crushing after sliding, and WC is web crushing without sliding.

In the ACI 349 general and seismic provisions, the predicted shear strength underestimated the test results: V_{test}/V_n =1.33~1.80 (general provision), and V_{test}/V_{seis} =1.27~1.69 (seismic provision). In the calculation of the shear strength, the permissible maximum shear strength in Eq. (5) was applied.

In the Eurocode 8, the predicted shear strength is estimated by the minimum design strength considering three different failure modes: diagonal compression failure of the web (DC), diagonal tension failure of the web (DT), and sliding shear failure (SS). The predicted shear strengths significantly underestimated the test results: V_{test} / V_{RD} =1.72~2.63.

Gulec and Whittaker developed empirical equations to predict the shear strength of low-rise walls ($h_w / l_w \le 1.0$) with rectangular cross-sections and barbell-type sections. For this, statistical analysis was performed for existing test results of 434 walls [6]. The predictions by the Gulec and Whittaker equation were the best among the design equations, though the equation was based on the test results for the most of Grade 420 MPa or less bars: V_{test} / V_{Wh} =1.00~1.36.

A computer software RCAHEST [7], [8] was used for nonlinear finite element analysis of the test specimens. The finite element analysis predicted the shear strength with good accuracy: V_{test} / V_{FE} =0.88~1.02.

5. Conclusion

To verify the validity of Grade 550 MPa re-bars for shear reinforcement of low-rise walls, four wall specimens with $h_w / l_w = 1.0$ were tested under cyclic lateral loading. Specimens **S1**~**S4** were designed to fail by shear, by intentionally increasing the flexural strength. Using the test results, the validity of the current shear design equations is evaluated for Grade 550 MPa bars.

The major findings of the present study are summarized as follows.

- The failure of Specimens **S1**, **S2**, and **S3** without boundary confinement occurred due to sliding of the panel (along the diagonal cracks) followed by web crushing, while the failure of Specimen **S4** with boundary confinement occurred due to web crushing without sliding of panel.
- The maximum shear strength V_{test} was significantly greater than the predictions by the ACI 349 (ACI 318) general and seismic provisions: V_{test} / V_n =1.33~1.80 (general provision), and V_{test} / V_{seis} =1.27~1.69 (seismic provision). In all specimens, at least one of the horizontal bars yielded before the failure of the walls.
- Direct comparison of **S1** and **S2**, which had similar $A_s f_y$ and f_c', but different bar grade for horizontal reinforcement (i.e. **S1** with Grade 550 MPa bars and **S2** with Grade 420 MPa bars), showed that in both specimens, the damage and failure modes were identical. On the other hand, the maximum strength of **S1** was 6% less than that of **S2** (V_{test} / V_n for **S1** and 1.75 for **S2).** The lesser shear strength of **S1** is attributed to the increased diagonal crack width, which was caused by the smaller area and greater spacing of the high strength horizontal bars.
- Eurocode 8 shear provision significantly underestimated the shear strength of the specimens: V_{test} / V_{RD} =1.72~2.63. The predictions by the Gulec and Whittaker equation were the best among the design equations: V_{test} / V_{Wh} =1.00~1.36. The finite element analysis predicted the shear strengths with good accuracy: V_{test} / V_{FE} =0.88~1.02.

6. Acknowledgements

This work was supported by the Power Generation & Electricity Delivery of the Korea Institute of Energy Technology Evaluation and Planning (KETEP) grant funded by the Korea government Ministry of Knowledge Economy (No. 2011T100200162).

7. References

[1] ACI 318 Committee. Building Code Requirements for Structural Concrete (ACI 318-11) and Commentary. *American Concrete Institute*. Farmington Hills, 2011.

[2] ACI 349 Committee. Code Requirements for Nuclear Safety-Related Concrete Structures (ACI 349 M-06) and Commentary. *American Concrete Institute*. Farmington Hills, 2006.

[3] N. M. Hawkins, and S. K. Ghosh. Acceptance Criteria for Special Structural Walls Based on Validation Testing. Proposed Provisional Standard and Commentary. *S.K. Ghosh Associates Inc*. Northbrook, IL, 2003.

[4] British Standards Institution. Eurocode 8: Design of Structures for Earthquake Resistance EN1998-1: 2004. *Brussels: CEN- European Committee for Standardization*, 2004.

[5] C. K. Gulec, and A. S. Whittaker. Empirical Equations for Peak Shear Strength of Low Aspect Ratio Reinforced

Concrete Walls. *ACI Structural Journal.* V. 108. No. 1. January-February 2011, pp. 80-89.

[6] C. K. Gulec, and A. S. Whittaker Performance-Based Assessment and Design of Squat Reinforced Concrete Shear Walls. *Multidisciplinary Center for Earthquake Engineering Research, Buffalo, NY*. Technical Report MCEER-09-0010. 2009.

[7] T. H. Kim, H. K. Hong, Y. S. Chung, and H. M. Shin. Seismic performance assessment of reinforced concrete bridge columns with lap splices using shaking table tests. 2009, *Magazine of Concrete Research* 61(9): pp. 705-719.

[8] H. Okamura, K. Maekawa, and S. Sivasubramaniyam. Verification of Modeling for Reinforced Concrete Finite Element. Finite Element Analysis of Reinforced Concrete Structures, *Journal of Structural Engineering*, ASCE. 1985.